Chemical Physics Letters 742 (2020) 137128

Contents lists available at ScienceDirect

Chemical Physics Letters

journal homepage: www.elsevier.com/locate/cplett

Research paper

Structural, optical, thermal and nonlinear optical properties of Triphenylamine (TPA) single crystal grown by Bridgman – Stockbarger method

K. Ramachandran[a,*], Arumugam Raja[a], N. Lingamurthy[b], Muthu Senthil Pandian[a], P. Ramasamy[a], S. Venugopal Rao[b]

[a] SSN Research Centre, SSN College of Engineering, Chennai 603 110, Tamilnadu, India
[b] Advanced Centre of Research in High Energy Materials (ACRHEM), University of Hyderabad, Hyderabad 500 046, Telangana State, India

HIGHLIGHTS

- Organic nonlinear optical Triphenylamine single crystal has been grown from Bridgman – Stockbarger method.
- The excellent optical transmittance of TPA single crystal has been observed in the near infrared region (82%).
- Thermal stability of TPA single crystal has been observed upto 140 °C.

ARTICLE INFO

Keywords:
TPA crystal
Bridgman – Stockbarger
UV–Vis NIR
TG-DTA
Nonlinear optical

ABSTRACT

Optically transparent Triphenylamine (TPA) single crystal has been grown by Bridgman-Stockbarger method. Phase confirmation of TPA crystal was investigated using SXRD and PXRD analyses. Hirshfeld Surface was performed on TPA. The chemical bonding structure of TPA has been obtained from the FTIR spectral study. Optical transmittance properties of the grown crystal were obtained from the UV–Visible NIR spectrum analysis. Thermal properties of the TPA single crystal were identified using TG-DTA analyser. Q-switched Nd:YAG laser (λ = 1064 nm) has been used for the LDT measurement. Second harmonic generation of organic TPA crystal was analysed by Kurtz- Perry powder technique.

1. Introduction

The organic materials are used for several technological applications such as, optical telecommunication, optical data storage, laser frequency conversion, color displays and etc [1–6]. The organic materials exhibit ultrafast nonlinear optical response, large optical susceptibility, large hyperpolarizability and high laser damage threshold compared to inorganic materials. The good performance of nonlinear optical materials need several conditions such as, the large nonlinear optical coefficient, phase matchability, good optical transmittance, high laser damage threshold, high thermal conductivity, machinability and moderate birefringence [7–10]. Especially, the nonlinear optical single crystals are having good optical transmittance in the visible to near infrared region and superior second harmonic generation (SHG) efficiency. New organic materials suitable for optoelectronic and photonic device applications are being explored [11].

In general, Triphenylamine (TPA) is a well known organic material and its derivatives were frequently used for numerous applications such as, organic light emitting diodes, solar cells and photoconductors [12] as well as second order nonlinear optical applications. Further, the TPA group of materials possess electron donating character, because they have electron rich nitrogen atom interconnected with three phenyl groups [13]. The synthesis of triphenylamine molecule was obtained from the different kind of methods and the physical and chemical properties of the synthesized TPA material were carried out using different characterization techniques [14]. The crystal structure and carrier transport properties of Triphenylamine derivative single crystals were reported by several authors [15–16]. Triphenylamine single crystal with excellent photoconducting property was grown in helium atmosphere using Bridgman method [17]. Experimental and theoretical Fourier transform infrared (FTIR) spectrum and molecular structure of the present molecule were reported by Reva et al.

* Corresponding author.
E-mail address: ramphy18@gmail.com (K. Ramachandran).

https://doi.org/10.1016/j.cplett.2020.137128
Received 12 October 2019; Received in revised form 13 January 2020; Accepted 17 January 2020
Available online 19 January 2020

However, in the present work, the bulk size, good quality and optically transparent organic TPA single crystal has been grown using Bridgman –Stockbarger method under vacuum. The grown TPA single crystals were subjected to structural (SXRD, PXRD and FTIR) Optical (UV–Visible, Photoluminescence (PL), Birefringence and SHG), laser damage threshold (LDT) and thermal (TG-DTA) characterizations.

2. Experimental method

High purity (99.9%) triphenylamine compound was obtained from Alfa Aesar. The details about the growth ampoule design were discussed in the previously reported article [2]. The title material was loaded in borosilicate growth ampoule. The growth ampoule was evacuated upto the range of 2×10^{-6} milli bar using Hind High Vacuum (HHV) system. The growth ampoule was placed in the maximum temperature of the homemade single zone transparent Bridgman-Stockbarger furnace. The temperature was gradually increased from room temperature to the melting point of triphenylamine compound (M.P – 129 °C) and further, the temperature was raised in excess of melting point by 3 °C. The optimized growth condition was observed at 0.75 mm / hour and it is translated using nano stepper motor. Finally, the optically transparent and defect free TPA single crystal was grown using Bridgman – Stockbarger method. The grown single crystal was carefully removed from the growth ampoule using diamond wheel cutter. Fig. 1(a) shows the optically transparent as grown TPA single crystal and Fig. 1(b) displays the cut and polished TPA crystal wafers.

3. Material characterization

Crystal structure and lattice parameters of TPA single crystal were investigated via the Bruker AXS Kappa APEX II single crystal X-ray diffractometer and MoKα (λ = 0.710 Å) is used as a monochromator source for X-ray radiation. Crystalline nature of TPA single crystal was explored using PANalytical Empyrean X-ray diffractometer with CuKα (λ = 1.5406 Å) and it was scanned (2θ degree) ranging from 5° to 50°. The crystal bonding structure was investigated using Fourier transform infrared (FTIR) spectrum with KBr Pellet technique. FTIR spectral wavelength range was obtained from 4000 – 500 cm^{-1}. Optical transmittance and cut off wavelength of TPA crystal were analysed by Perkin-Elmer lambda 35 spectrophotometer. UV–Visible spectrum was taken for the range 200–1100 nm and the sample of TPA was of thickness – 1.5 mm. The photoluminescence properties of TPA material were investigated using Jobin Yvon Fluorolog - Fl3-11 spectroflurometer with Xenon lamp source at 450 W. The resolution of specific wavelengths was observed at 0.2 nm. Thermal properties were measured for TPA crystal by the TG-DTA measurement (Perkin–Elmer Diomand TG/DTA analyser). The laser damage threshold measurement of TPA single crystal was carried out using Q-switched Nd:YAG nanosecond laser, INNOLAS Spit Light, 1.2 J @ 1064 nm. The nonlinear optical property was investigated using Kurtz -Perry powder technique.

Table 1
The lattice parameters of the TPA single crystal.

Cell Parameters	Reported [18]	Present Work
a	15.49 Å	15.74 Å
b	15.63 Å	15.97 Å
c	22.06 Å	22.49 Å
α	90°	90°
β	90.95°	91°
γ	90°	90°
Volume (V)	5340 $Å^3$	5653 $Å^3$
Crystal System	Monoclinic	Monoclinic
Space group	Cc	Cc

4. Results and discussion

4.1. Structural properties

4.1.1. Single crystal X-ray diffraction study

Crystal structure, space group, bond length, bond angle, atom position and lattice parameters of the grown TPA single crystal were measured using single crystal X-ray diffraction (SXRD) study. The grown TPA single crystal possesses monoclinic crystal system with non-centrosymmetric space group of Cc, which is obtained from the lattice parameter values and the results are compared with the earlier results reported in literature [18]. These values are in close agreement and the details are given in Table 1 and three dimensional molecular packing structure of TPA crystal viewed through 'b' axis is shown in Fig. S1.

4.1.2. Powder X-ray diffraction study

Phase purity and lattice parameters of TPA were investigated using powder X-ray diffraction (PXRD) analysis. Powder X-ray diffraction study reveals the good crystalline nature and lattice parameters of the TPA crystal. The obtained hkl values are (1 1 0), (1 1 1), (0 2 0), (2 2 0), (1 3 0), (2 2 –3), (3 1 –3), (4 0 0), (0 0 6), (4 2 1), (3 1 –6), (1 5 3) and (2 2 9). Theoretical X-ray diffraction peaks were obtained from the standard crystallographic information file (CIF Number − 660 790) using Mercury 3.8 software. Fig. 2 divulges the powder X-ray diffraction of TPA crystal. These diffraction peaks were compared with experimental X-ray diffraction results. Subsequently, these diffraction peaks of TPA molecule closely matched with theoretical values and the lattice parameter values are obtained from the following expression,

$$\frac{1}{d^2} = \frac{1}{\sin^2\beta}\left(\frac{h^2}{a^2} + \frac{k^2\sin^2\beta}{b^2} + \frac{l^2}{c^2} - \frac{2hl\cos\beta}{ac}\right) \quad (1)$$

The lattice parameter values are a = 15.49 Å, b = 15.69 Å, c = 22.37 Å and these values agree with the previously reported values in literature [18].

4.1.3. Hirshfeld surface plot

The intermolecular interactions / contacts (Hirshfeld surfaces and 2D fingerprint plots) of TPA molecule were investigated from the

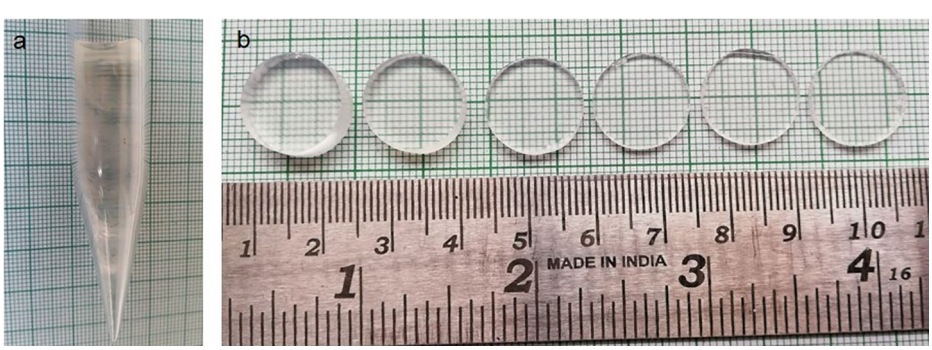

Fig. 1. (a) As grown and (b) cut and polished TPA crystals.

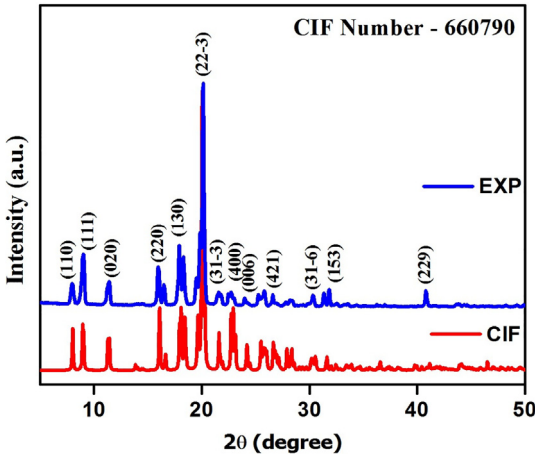

Fig. 2. Powder X-ray diffraction of TPA crystal.

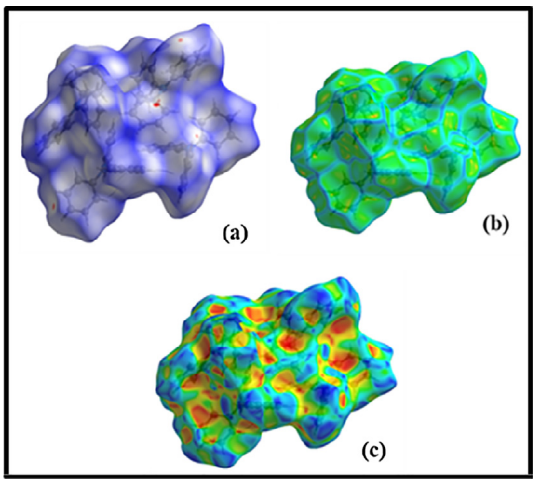

Fig. 3. Hirshfeld surface of (a) d_{norm} (-0.068 to 1.243), (b) curvedness (-4.000 to 0.400) and (c) shape index (-1.000 to 1.000).

Crystal Explorer 3.1 software and it is interpreted by the single crystal X-ray diffraction studies (CIF Number: 660790). Fig. 3 shows the Hirshfeld surface of TPA molecule and this molecule was generated using the crystal explorer and it displays (a) d_{norm} (−0.068 to 1.243), (b) curvedness (−4.000 to 0.400) and (c) shape index (−1.000 to 1.000). The d_{norm} value is negative, which represents the shorter contacts and the d_{norm} value is positive, which represents the intermolecular contacts of the present molecule is longer. The red color indicates the shorter contacts for negative, the blue color indicates the longer contacts for positive and the white color indicates that the d_{norm} value is exactly zero. The shape index is more sensitive and slight changes have been observed in the surface shape of TPA crystal. The value of the curvedness is calculated from the flat surface area of the molecule which corresponds to low values of curvedness. High values of the curvedness are related to sharp curvature areas of the molecule and the corners sepearate the surface into areas indicating the interactions between the neighbouring molecules [19–21].

The 2D fingerprint plots were translated for 1.0 – 2.8 Å, d_e and d_i are distance scales of the graph axes. Fig. S2 (i-vii) shows the two-dimensional fingerprint plot of the TPA molecule and it exhibits that the over all contribution, C···C, C···H, H···H, H···N, N···H and H···C and all these intermolecular contacts are highlighted separately in 2D fingerprint plots. From the fingerprint analysis, the total molecular interaction was observed at 100%. From the crystal structure, the major contribution of H···H (68.1%) bonding interactions is high compared to other intermolecular interactions of C···C (0.5%), C···H (16.7%), H···N (0.1%) N···H (0.1%) and H···C (14.6%). From the results, it can be concluded that the strongest intermolecular interaction of the present molecule was found to be H···H (68.1%), which is obtained from the crystal explorer.

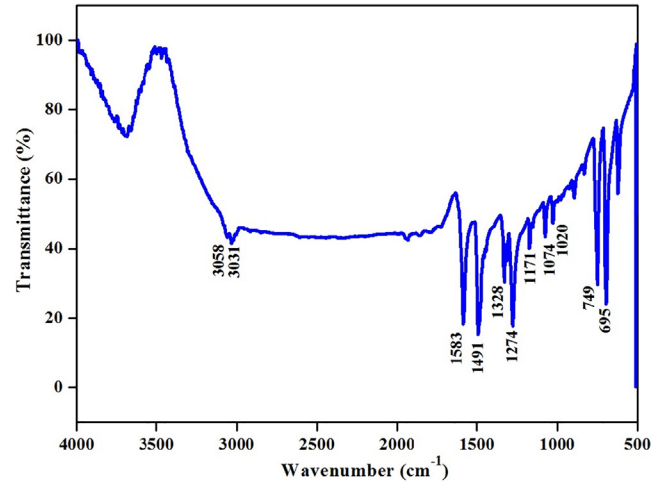

Fig. 4. FTIR spectrum of TPA.

4.2. Vibrational analysis

The infrared light passes through the materials and it gives the information about the fundamental vibration, bond strength, bond type and molecular structure [22]. The chemical bonding structure was investigated using KBr pellet technique within the wavenumber ranges from 500 to 4000 cm^{-1}. The obtained vibrational spectrum of TPA material is shown in Fig. 4. The aromatic C—H stretching peaks were observed at 3058 and 3031 cm^{-1} [23]. The strongest phenyl ring (C═C) appeared at 1583 and 1491 cm^{-1}, which could contribute to monosubstituted benzene derivatives [12]. The strongest peaks appeared at 1328 and 1274 cm^{-1}, which can be attributed to C—N stretching vibrations [24]. The low intensity peaks were observed at 1171, 1074 and 1020 cm^{-1}, due to the presence of aromatic C—H in-plane bending vibrations [12,24]. The fundamental vibration peaks were observed at 695 and 749 cm^{-1}. It could be attributed to the aromatic C—H out of plane bending vibrations [22,25].

4.3. UV–Visible NIR spectrum analysis

Organic single crystals should possess good optical transmittance and little absorption in the visible to near infrared region [26–27]. The extinction coefficient, refractive index and optical absorption coefficient of organic single crystal were determined using optical study and these results were used for the optical applications [22]. The obtained optical transmittance spectrum of TPA crystal is shown in Fig. 5. Fig. 5 shows the good optical transmittance at 82% in the infrared region. The optical cut-off wavelength is observed at 368 nm and the excellent optical transmittance was got in the range of 368 nm to 1100 nm, which is more than 60% optical transmittance in the visible to infrared region. Before cut off wavelength of TPA single crystal (368 nm), the optical transmittance suddenly decreased, due to the presence of π–π* and n–π* electronic transition [7]. The optical bandgap energy was calculated using the following expression,

$$E_g = \frac{hc}{\lambda_e} \tag{2}$$

where λ is the cut-off wavelength, h is the Plancks constant and c is the velocity of light.

The optical absorption coefficient can be calculated from the optical transmittance and the crystal thickness of TPA crystal and it was

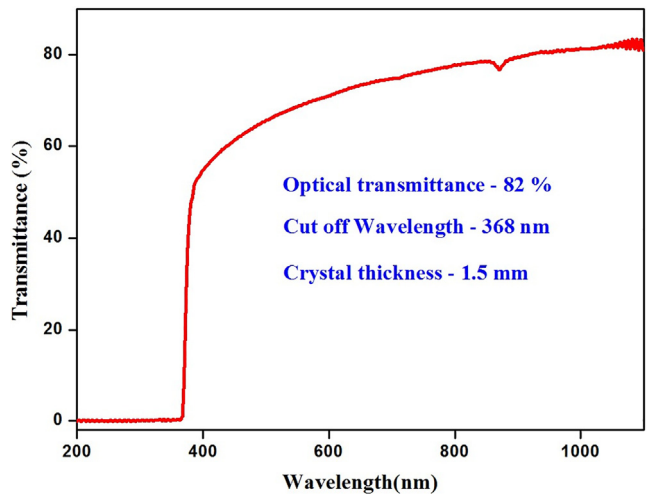

Fig. 5. Optical transmittance of TPA single crystal.

determined by the following relation [5],

$$\alpha = \frac{2.303}{t}\log_{10}\left(\frac{100}{T}\right) \tag{3}$$

where α is an optical absorption coefficient, T is optical transmittance and t is the crystal thickness. The optical transmittance and optical absorption coefficient values of TPA crystal can be used to calculate the optical bandgap energy and it is evaluated from the following expression,

$$\alpha h\upsilon = A(h\upsilon - E_g)^m \tag{4}$$

where ν is the frequency of the incident photons, E_g is the optical bandgap, A is optical constant and m values are 1/2 and 2 for direct and indirect transtitions, respectively. The optical bandgap energy value is calculated using the photon energy (hν) versus $(\alpha h\nu)^2$ and it is shown in Fig. S3. The direct optical bandgap energy value was obtained by extrapolating the linear part of the y-axis to the energy axis. The obtained tauc plot graph and theoretically calculated optical bandgap energy value is same and the value was found to be 3.35 eV.

4.4. Photoluminescence study

Photoluminescence is used to study the several properties such as, surface defects, oxygen vacancies, charge carrier separation, recombination mechanism and color centre of the material [28]. At room temperature, the excitation and emission properties of TPA molecule were examined via PL analysis. The TPA material was excited at 323 nm and the corresponding emission was recorded in the range of 340 nm to 620 nm. The photoluminescence of TPA crystal is shown in Fig. 6. The corresponding broad centre emission peak was observed at 377 nm, which is attributed to n → π* transition state [29].

4.5. Thermal properties

Thermogravimetric and differential thermal analysis (TG-DTA) reveals the thermal stability and melting point of the materials. The TPA sample was taken in the alumina crucible and the sample weight of 6.117 mg was used. Heating rate of the sample is 5 °C per minute. The nitrogen (N_2) atmosphere was used for this experiment. The crystal sample was heated from room temperature (RT) to 270 °C. The thermal property of TPA single crystal is shown in Fig. 7. It clearly shows that the thermal stability of TPA crystal was observed upto 140 °C. Furthermore, the temperature was increased upto 270 °C. Single stage weight loss is observed after 140 °C upto 236 °C. From the DTA graph, the sharp endothermic peak was observed at 129 °C, which confirms the melting point of the TPA material.

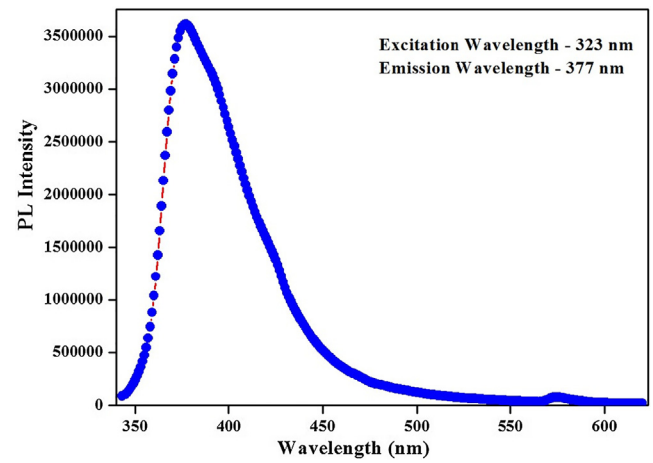

Fig. 6. The emission spectrum of TPA crystal.

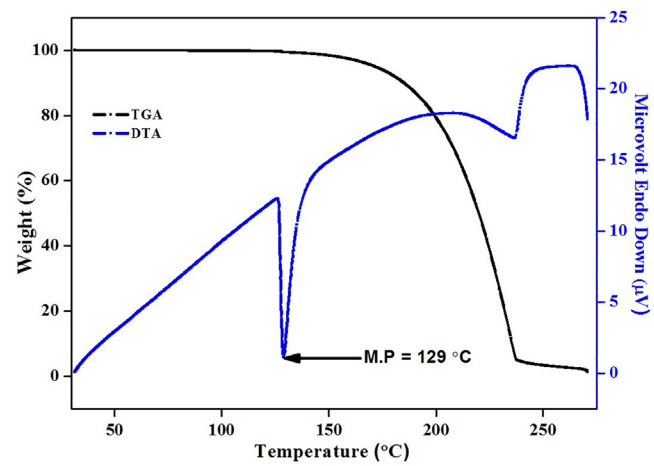

Fig. 7. Thermal stability of TPA.

4.6. Birefringence study

Optical homogeneity of the grown TPA single crystal has been determined from the Birefringence interferometry. The birefringence value is the difference between the two refractive indices of ordinary (o-ray) and extraordinary (e-ray) [30]. Most of the birefringence single crystals can be attractive for optical applications such as, calculators, beamsplitter and polarisers etc [31]. The birefringence experiment was already reported by several authors [32,33]. The cut and polished smooth surface (crystal thickness – 1 mm) of the TPA crystal and He-Ne laser (5 mW) of wavelength 632.8 nm were used for this experiment. Two fringes were observed at birefringence interferogram. The birefringence value was calculated using the following relation [30],

$$\nabla n = \frac{K\lambda}{t} \tag{5}$$

where K is the order of fringes, λ is the wavelength of laser light and t is the thickness of crystal. In this present work, the calculated birefringence value is 0.001265. The crystal optic axis and crystal phase matching angle of the present crystal were determined from the Birefringence interferometer. The obtained birefringence value of the TPA is compared with the other organic/inorganic materials [30 –35] and the values are tabulated in Table S1.

4.7. Laser damage threshold

Surface laser damage threshold of organic / inorganic and semiorganic single crystals have been more attractive in the several processes like electron avalanche, multi-photon absorption, thermal absorption, photochemical dissociation, electrostrictive fracture and etc [36]. The LDT experiment was assessed by the two way process. (i) single shot mode and (ii) multiple shot mode. In present investigation, the pulse width of the laser was 7 ns. The pulse repetition rate was fixed at 10 Hz and also the input laser beam diameter is measured as 8 mm. The good quality and circular shape of cut and polished TPA single crystal of thickness 4 mm was selected for LDT measurement. In single shot mode (wavelength of laser = 532 nm in operating mode), the incident energy (in millijoule) applied into TPA single crystal was measured using attenuator. The focal length of plano-convex lens is observed at 10 cm and it could be attached at the translation stage of sample holder. The translation stage (X-Y plane) was adjusted using ESP 300 controller. The surface laser damage threshold was obtained from the power meter and it can be calculated from the following expression [37],

$$\text{Power density}\,(P_d) = \frac{E}{\tau\pi\,(\omega_z{}^2)}\left(\frac{GW}{cm^2}\right) \tag{6}$$

where E is the input energy of laser beam (mJ), τ is the pulse width of laser (ns) and ω_z is the radius of the laser beam. The radius of the laser beam (ω_z) was calculated using the following relation,

$$\omega_z = \omega_0\sqrt{1 + \left(\frac{Z}{Z_R}\right)^2} \tag{7}$$

$$Z_R = \left(\frac{\pi\omega_0{}^2}{\lambda}\right);\ \omega_0 \geqslant \frac{2\lambda}{\pi} \tag{8}$$

$$\omega_0 = \left(\frac{2\lambda}{\pi}\right)\left(\frac{f}{d}\right) \tag{9}$$

where λ., the laser wavelength, is 532 nm and d is the laser beam diameter 8 mm. The experimental (ω_0) value was calculated at 10×10^{-6} m using the knife edge measurement. The Rayleigh length *(Z_R)* was measured as 590 μm. Finally, radius of the laser beam (ω_z) was evaluated from the above Eq. (7) and it can be measured at 85.3 μm. The single shot laser energy (2 mJ) was applied into the grown organic single crystal, which resulted in small dot appearing on the crystal surface. The LDT value was found to be 1.25 GW/cm^2 (2 mJ). Fig. S4 shows the optical microscope image of damage pattern in TPA crystal. The laser damage threshold of TPA value is compared with other standard single crystals [2,5,37–40]. However, comparing these values is not accurate because the testing conditions are different (pulse width, wavelength of laser and spot size etc) and it is tabulated in Table S2. The grown organic TPA single crystal can be used for high tech laser and it also can be used for NLO applications like mode locking, photonics, optical limiting, data processing and SHG devices [38].

4.8. Nonlinear optical study

The nonlinear optical property of the TPA crystal was investigated using the Kurtz-Perry powder technique and it is an impotant technique to evaluate the second harmonic conversion efficiency of nonlinear single crystals. The crushed TPA powder material (Homogeneous particle size) was tightly packed in microcapillary tube of 1 mm diameter. A Q-switched Nd:YAG laser source at the fundamental wavelength of 1064 nm and the output energy of the emitted green wavelength of 532 nm was used. The pulse width and pulse repetition rate were 10 ns and 10 Hz, respectively. The focal length of the plano-convex lens is 20 cm [41]. A Q-switched Nd:YAG laser light (input energy 1.2 mJ/pulse) was passed through the randomly oriented organic TPA crystals and it was focused by the focal length of the plano-convex lens before sample holder. The output voltage signals of second harmonic generation light were detected using photomultiplier tube (PMT) which is interconnected with digital storage oscilloscope. Finally, the SHG output signal voltage was measured from the digital storage oscilloscope. The second harmonic was generated and it was confirmed through the emission of bright green light. In this work, the potassium dihydrogen phosphate (KDP) material (80 mV) was used as a standard reference material having homogeneous particle size. Second harmonic generation of output signal voltage is found to be 16 mV. Hence, the organic crystal is moderately useful for nonlinear optical applications.

5. Conclusion

Good quality and optically transparent Triphenylamine single crystal (TPA) was grown by Bridgman - Stockbarger method. Crystal structure and lattice parameters of TPA single crystal were confirmed through X-ray diffraction analysis. Hirshfeld surface and Finger print plot were obtained from the crystal explorer software. The aromatic C—H in plane and out of plane bending vibrations were analysed through the FTIR spectrum. Optical transmittance and cut-off wavelength of the grown organic TPA single crystal were analysed. Thermal stability of TPA material is observed upto 140 °C. Melting point of the TPA crystal is obtained at 129 °C. The excitation and emission property of TPA material was studied using photoluminescence spectrum. Birefringence value of the present crystal has been compared with standard crystals. Surface laser damage threshold is observed at 1.25 GW/cm^2. SHG output signal voltage of organic TPA single crystal was found to be 16 mV.

Credit authorship contribution statement

K. Ramachandran: writing - original draft. **Arumugam Raja:** writing review & Editing. **N. Lingamurthy:** Data curation. **Muthu Senthil Pandian:** Investigation. **P. Ramasamy:** Supervision. **S. Venugopal Rao:** Formal Analysis.

Declaration of Competing Interest

The authors declare that they have no known competing financial interests or personal relationships that could have appeared to influence the work reported in this paper.

Acknowledgment

One of the authors (K. Ramachandran) thanks SSN Management for providing Junior Research Fellowship (JRF).

Appendix A. Supplementary material

Supplementary data to this article can be found online at https://doi.org/10.1016/j.cplett.2020.137128.

References

[1] N.V. Sonia, M. Vij, K. Thukral, N. Khan, D. Haranath, M.S. Rajnikant, Investigation on the key aspects of l-arginine para nitrobenzoate monohydrate single crystal: a non-linear optical material, Chin. J. Chem. Eng. 27 (2019) 701.
[2] K. Ramachandran, Arumugam Raja, V. Mohankumar, Muthu Senthil Pandian, P. Ramasamy, Growth and characterization of 4-methyl-3-nitrobenzoic acid (4M3N) single crystal by using vertical transparent Bridgman-Stockbarger method for NLO applications, Phys. B. 562 (2019) 82.
[3] Zhihua Sun, Guanghui Zhang, Xinqiang Wang, Zeliang Gao, Xiufeng Cheng, Shaojun Zhang, Dong Xu, Growth, morphology, thermal, spectral, linear, and nonlinear optical properties of l-Arginine Bis (trifluoroacetate) crystal, Cryst. Growth Des. 9 (2009) 3251.
[4] Honghong Chen, Qi Ma, Yuqiao Zhou, Zhou Yang, Mojca Jazbinsek, Yongzhong Bian, Ning Ye, Dong Wang, Hui Cao, Wanli He, Engineering of organic chromophores with large second-order optical nonlinearity and superior crystal growth ability, Cryst. Growth Des. 15 (2015) 5560.

[5] K. Ramachandran, Arumugam Raja, V. Mohankumar, Muthu Senthil Pandian, P. Ramasamy, Experimental and theoretical approach of organic 4,4′-dimethylbenzophenone (DMBP) single crystal for NLO application, Opt. Laser Technol. 119 (2019) 105640.

[6] R. Sankar, C.M. Raghavan, M. Balaji, R. Mohan Kumar, R. Jayavel, Synthesis and growth of triaquaglycinesulfatozinc (II),$[Zn(SO_4)(C_2H_5NO_2)(H_2O)_3]$, a new semi-organic nonlinear optical crystal, Cryst. Growth Des. 7 (2007) 348.

[7] Huaihong Zhang, Yu Sun, Xiaodan Chen, Xin Yan, Baiwang Sun, Crystal growth and characterization of organic single crystal: N-(2-hydroxybenzylidene) acetohydrazide, J. Cryst. Growth. 324 (2011) 196.

[8] Z.H. Sun, G.H. Zhang, X.Q. Wang, X.F. Cheng, X.J. Liu, L.Y. Zhu, H.L. Fan, G. Yu, D. Xu, Growth and characterization of the nonlinear optical single crystal: l-lysine acetate, J. Cryst. Growth. 310 (2008) 2842.

[9] Guangfeng Liu, Jie Liu, Xiaoxin Zheng, Yang Liu, Dongsheng Yuan, Xixia Zhang, Zeliang Gao, Xutang Tao, Bulk crystal growth and characterization of semi-organic nonlinear optical crystal tri-diethylammonium hexachlorobismuthate (TDCB), CrystEngComm 17 (2015) 2569.

[10] D. Balasubramanian, R. Sankar, V. Siva Shankar, P. Murugakoothan, P. Arulmozhichelvan, R. Jayavel, Growth and characterization of semiorganic nonlinear optical rubidium bis-dl-malato borate single crystals, Mater. Chem. Phys. 107 (2008) 57.

[11] S. Anbu Chudar Azhagan, S. Ganesan, Effect of zinc acetate addition on crystal growth, structural, optical, thermal properties of glycine single crystals, Arab. J. Chem. 10 (2017) S2615.

[12] Igor Reva, Leszek Lapinski, Nitin Chattopadhyay, Rui Fausto, Vibrational spectrum and molecular structure of triphenylamine monomer: A combined matrix-isolation FTIR and theoretical study, Phys. Chem. Chem. Phys. 5 (2003) 3844.

[13] Geunseok Jang, Jongho Kim, Daigeun Kim, Taek Seung Lee, Synthesis of triphenylamine-containing conjugated polyelectrolyte and fabrication of fluorescence color-changeable, paper-based sensor strips for biothiol detection, Polym. Chem. 6 (2015) 714.

[14] Touraj Manifar, Sohrab Rohani, Synthesis and analysis of triphenylamine: a review, Can. J. Chem. Eng. 82 (2004) 323.

[15] Minoru Umeda, Mitsuhiko Katagiri, Sayoko Shironita, Norio Nagayama, Anisotropic surface hole-transport property of triphenylamine-derivative single crystal prepared by solution method, Appl Surf Sci. 388 (2016) 109.

[16] Motoki Kunihiro, Yasuaki Nakasone, Shofu Matsuda, Sayoko Shironita, Norio Nagayama, Minoru Umeda, Crystal structure oriented carrier transport characteristic of triphenylamine derivative single crystal, AIP Adv. 8 (2018) 035324.

[17] D.C. Hoesterey, G.M. Letson, Hole photoconductivity in ferrocene, triphenylamine, and trans-stilbene, J. Chem. Phys. 41 (1964) 675.

[18] E. Martin, C.R. Pulham, S. Parsons, CCDC 660790: Experimental Crystal Structure Determination, 2008.

[19] J. McKinnon Joshua, Dylan Jayatilaka, Mark A. Spackman, Towards quantitative analysis of intermolecular interactions with Hirshfeld surfaces, Chem. Commun. 37 (2007) 3814.

[20] Yang-Hui Luo, Bai-Wang Sun, Two new metastable forms of 6-chloroquinolin-2 (1H)-one: Crystal structure, Hirshfeld surfaces and spectroscopic studies, Spectrochim. Acta A. 120 (2014) 381.

[21] J.J. McKinnon, F.P. Fabbiani, M.A. Spackman, Comparison of polymorphic molecular crystal structures through Hirshfeld surface analysis, Cryst. Growth Des. 7 (2007) 755.

[22] Sahil Goel, Nidhi Sinha, Harsh Yadav, Abhilash J. Joseph, Abid Hussain, Binay Kumar, Optical, piezoelectric and mechanical properties of xylenol orange doped ADP single crystals for NLO applications, Arab. J. Chem. (2017).

[23] T. Arivazhagan, S. Siva Bala Solanki, Narayana Perumal Rajesh, "Investigation on crystal growth and characterization of organic nonlinear optical triphenylmethane single crystal by vertical Bridgman technique", J. Cryst. Growth. 496 (2018) 43.

[24] V. Govindan, D. Joseph Daniel, H.J. Kim, K. Sankaranarayanan, Crystal growth and characterization of 1, 3, 5-triphenylbenzene organic scintillator crystal, Mater. Chem. Phys. 223 (2019) 183.

[25] R. Subramaniyan@ Raja, G. Anandha Babu, P. Ramasamy, Studies on the growth and characterization of an organic single crystal–1, 3, 5-Triphenylbenzene, Mater. Res. Innov. 22 (2018) 1.

[26] Anuj Krishna, N. Vijayan, Chandan Bagdia, Kanika Thukral, D. Haranath, K.K. Maurya, G. Bhagavannarayana, Effect of ampoule support on the growth of organic benzimidazole single crystals by vertical Bridgman technique for nonlinear optical applications, CrystEngComm 18 (2016) 4844.

[27] Min Zhang, Xin Su, Shilie Pan, Zheng Wang, Hui Zhang, Zhihua Yang, Bingbing Zhang, Lingyun Dong, Ying Wang, Fangfang Zhang, Yun Yang, Linear and nonlinear optical properties of $K_3B_6O_{10}Br$ single crystal: experiment and calculation, J. Phys. Chem. C. 118 (2014) 11849.

[28] S. Kalaiyarasi, I.M.D. Zahid, S. Reena Devi, R. Mohan Kumar, Studies on the growth aspects, structural and third-order nonlinear optical properties of Piperidinium 3-carboxy-4-hydroxy benzenesulfonate single crystal, J. Cryst. Growth. 460 (2017) 105.

[29] Chil Won Lee, Ji-Young Kim, Myoung-Seon Gong, Jun Yeob Lee, Synthesis and photophysical properties of host materials with high triplet energy based on dibenzofuran and triphenylamine functionalities, Synth. Met. 162 (2012) 2059.

[30] N. Vijayan, K. Nagarajan, Alex M.Z. Slawin, C.K. Shashidharan Nair, G. Bhagavannarayana, Growth of benzimidazole single crystal by Sankaranarayanan − Ramasamy method and its characterization by high-resolution X-ray diffraction, thermogravimetric/differential thermal analysis, and birefringence studies, Cryst. Growth Des. 7 (2007) 445.

[31] M. Senthil Pandian, K. Boopathi, P. Ramasamy, G. Bhagavannarayana, The growth of benzophenone crystals by Sankaranarayanan-Ramasamy (SR) method and slow evaporation solution technique (SEST): A comparative investigation, Mater. Res. Bull. 47 (2012) 826.

[32] P. Maadeswaran, S. Thirumalairajan, J. Chandrasekaran, Growth, thermal, optical and birefringence studies of semiorganic nonlinear optical thiosemicarbazide cadmium chloride monohydrate (TCCM) single crystals, Optik. 121 (2010) 773.

[33] S. Kar, Sunil Verma, K.S. Bartwal, Growth optimization and optical characteristics of Fe doped $LiNbO_3$ crystals, Cryst. Growth Des. 8 (2008) 4424.

[34] V. Vasudevan, R. Ramesh Babu, K. Ramamurthi, Unidirectional growth of l-lysine l-lysinium dichloride nitrate (l-LLDN) single crystals by the SR method, Phys. B. 406 (2011) 936.

[35] S. Dhanuskodi, J. Ramajothi, Crystal growth, thermal and optical studies of L-histidine tetrafluoroborate: a semiorganic NLO material, Cryst. Res. Tech. 39 (2004) 592.

[36] S. Vanishri, J.N. Babu Reddy, H.L. Bhat, S. Ghosh, Laser damage studies in nonlinear optical crystal sodium p-nitrophenolate dihydrate, Appl. Phys. B. 88 (2007) 457.

[37] P. Karuppasamy, T. Kamalesh, V. Mohankumar, S. Abdul Kalam, Muthu Senthil Pandian, P. Ramasamy, Sunil Verma, S. Venugopal Rao, Synthesis, growth, structural, optical, thermal, laser damage threshold and computational perspectives of 4-nitrophenol 4-aminobenzoic acid monohydrate (4NPABA) single crystal, J. Mol. Struct. 1176 (2019) 254.

[38] K. Naseema, Sarath Ravi, Rakhi Sreedharan, Studies on a novel organic NLO single crystal: L-asparaginium Oxalate, Chin. J. Phys. 60 (2019) 612.

[39] V. Venkataramanan, C.K. Subramanian, H.L. Bhat, Laser induced damage in zinc tris (thiourea) sulfate and bis (thiourea) cadmium chloride, J. Appl. Phys. 77 (1995) 6049.

[40] N. Vijayan, G. Bhagavannarayana, T. Kanagasekaran, R. Ramesh Babu, R. Gopalakrishnan, P. Ramasamy, Crystallization of benzimidazole by solution growth method and its characterization, Cryst. Res. Tech. 41 (2006) 784.

[41] S.K. Kurtz, T.T. Perry, A powder technique for the evaluation of nonlinear optical materials, J. Appl. Phys. 39 (1968) 3798.